

# Progress in Neutron EM Couplings

Igor Strakovsky<sup>1,a)</sup>, William Briscoe<sup>1</sup>, Alexander Kudryavtsev<sup>2,1</sup>, Viacheslav Kulikov<sup>2</sup>, Maxim Martemianov<sup>2</sup>, Vladimir Tarasov<sup>2</sup> and Ron Workman<sup>1</sup>

<sup>1</sup>*Department of Physics, The George Washington University, Washington, D.C. 20052, USA*

<sup>2</sup>*Institute of Theoretical and Experimental Physics, SRC “Kurchatov Institute”, Moscow 117218, Russia*

<sup>a)</sup>Corresponding author: igor@gwu.edu

**Abstract.** An overview of the GW SAID and ITEP groups' effort to analyze pion photoproduction on the neutron-target will be given. The disentanglement of the isoscalar and isovector EM couplings of  $N^*$  and  $\Delta^*$  resonances does require compatible data on both proton and neutron targets. The final-state interaction plays a critical role in the state-of-the-art analysis in extraction of the  $\gamma n \rightarrow \pi N$  data from the deuteron target experiments. Then resonance couplings determined by the SAID PWA technique are then compared to previous findings. The neutron program is important component of the current JLab, MAMI-C, Spring-8, ELSA, and ELPH studies.

## Introduction

The  $N^*$  family of nucleon resonances has many well established members [1], several of which exhibit overlapping resonances with very similar masses and widths but with different  $J^P$  spin-parity values. Apart from the  $N(1535)1/2^-$  state, the known proton and neutron photo-decay amplitudes have been determined from analyses of single-pion photoproduction. There are two closely spaced states above  $\Delta(1232)3/2^+$ :  $N(1520)3/2^-$  and  $N(1535)1/2^-$ . Up to  $W \sim 1800$  MeV, this region also encompasses a sequence of six overlapping states:  $N(1650)1/2^-$ ,  $N(1675)5/2^-$ ,  $N(1680)5/2^+$ ,  $N(1700)3/2^-$ ,  $N(1710)1/2^+$ , and  $N(1720)3/2^+$ . The present work reviews the region from the threshold to the upper limit of the SAID analyses, which is CM energy  $W = 2.5$  GeV.

One critical issue in the study of meson photoproduction on the nucleon comes from isospin. While isospin can change at the photon vertex, it must be conserved at the final hadronic vertex. Only with good data on both proton and neutron targets can one hope to disentangle the isoscalar and isovector electromagnetic (EM) couplings of the various  $N^*$  and  $\Delta^*$  resonances (see Refs. [2]), as well as the isospin properties of the non-resonant background amplitudes. The lack of  $\gamma n \rightarrow \pi^- p$  and  $\gamma n \rightarrow \pi^0 n$  data does not allow us to be as confident about the determination of neutron EM couplings relative to those of the proton. For instance, the uncertainties of neutral EM couplings of  $4^*$  low-lying  $N^*$  resonances,  $\Delta(nA_{1/2})$  vary between 25 and 140% while charged EM couplings,  $\Delta(pA_{1/2})$ , vary between 7 and 42%. Some of the  $N^*$  baryons [ $N(1675)5/2^-$ , for instance] have stronger EM couplings to the neutron relative to the proton, but the parameters are very uncertain [1]. One more unresolved issue relates to the second  $P_{11}$ ,  $N(1710)1/2^+$ . That is not seen in the recent  $\pi N$  partial-wave analysis (PWA) [3], contrary to other PWAs used by the PDG14 [1]. A recent brief review of its status is given in Ref. [4].

Additionally, incoherent pion photoproduction on the deuteron is interesting in various aspects of nuclear physics, and particularly, provides information on the elementary reaction on the neutron, i.e.,  $\gamma n \rightarrow \pi N$ . Final-state interaction (FSI) plays a critical role in the state-of-the-art analysis of the  $\gamma n \rightarrow \pi N$  interaction as extracted from  $\gamma d \rightarrow \pi NN$  measurements. The FSI was first considered in Refs. [5] as responsible for the near-threshold enhancement (Migdal-Watson effect) in the NN mass spectrum of the meson production reaction  $NN \rightarrow NNx$ . In Ref. [6], the FSI amplitude was studied in detail.

## Complete Experiment in Pion Photoproduction

Originally, PWA arose as the technology to determine amplitude of the reaction via fitting scattering data. That is a non-trivial mathematical problem – looking for a solution of ill-posed problem following to Hadamard and Tikhonov [7]. Resonances appeared as a by-product (bound states objects with definite quantum numbers, mass, lifetime and so on).

There are 4 independent invariant amplitudes for a single pion photoproduction. In order to determine the pion photoproduction amplitude, one has to carry out 8 independent measurements at fixed (s, t) (the extra observable is necessary to eliminate a sign ambiguity).

There are 16 non-redundant observables and they are not completely independent from each other, namely 1 unpolarized,  $d\sigma/d\Omega$ ; 3 single polarized,  $\Sigma$ ,  $T$ , and  $P$ ; 12 double polarized,  $E$ ,  $F$ ,  $G$ ,  $H$ ,  $C_x$ ,  $C_z$ ,  $O_x$ ,  $O_z$ ,  $L_x$ ,  $L_z$ ,  $T_x$ , and  $T_z$  measurements. Additionally, there are 18 triple-polarization asymmetries [9] (9 for linear (circular) polarized beam and 13 of them are non-vanishing) [8]. Obviously, the triple-polarization experiments are not really necessary from the theoretical point of view while such measurements will play a critical role to keep systematics under control.

## Neutron Database

Experimental data for neutron-target photoreactions are much less abundant than those utilizing a proton target, constituting only about 15% of the present worldwide known GW SAID database [9]. The existing  $\gamma n \rightarrow \pi^- p$  database contains mainly differential cross sections and 15% of which are from polarized measurements. At low to intermediate energies, this lack of neutron-target data is partially compensated by experiments using pion beams, e.g.,  $\pi^- p \rightarrow \gamma n$ , as has been measured, for example, by the Crystal Ball Collaboration at BNL [10] for the inverse photon energy  $E = 285 - 689$  MeV and  $\theta = 41^\circ - 148^\circ$ , where  $\theta$  is the inverse production angle of  $\pi^-$  in the CM frame. This process is free from complications associated with the deuteron target. However, the disadvantage of using the reaction  $\pi^- p \rightarrow \gamma n$  is the 5 to 500 times larger cross sections for  $\pi^- p \rightarrow \pi^0 n \rightarrow \gamma \gamma n$ , depending on  $E$  and  $\theta$ , which causes a large background, and there were no “tagging” high flux pion beams. Figures 1 and 2 summarize the available data for single

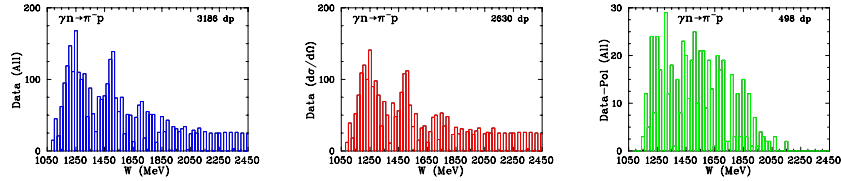


**FIGURE 1.** Data available for  $\gamma n \rightarrow \pi^- p$  as a function of CM energy  $W$  [9]. The number of data points, dp, is given in the upper right hand side of each subplot. The first subplot (blue) shows the total amount of  $\gamma n \rightarrow \pi^- p$  data available for all observables, the second subplot (red) shows the amount of  $d\sigma/d\Omega$  data available, the third subplot (green) shows the amount of polarization observables  $P$  data available.

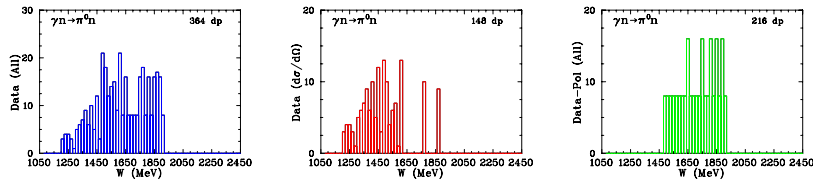


**FIGURE 2.** Data available for  $\gamma n \rightarrow \pi^0 n$  as a function of CM energy  $W$  [9]. Notation as in Fig. 1.

pion photoproduction on the neutron below  $W = 2.5$  GeV. Some high-precision data for the  $\gamma n \rightarrow \pi^- p$  and  $\gamma n \rightarrow \pi^0 n$  reactions have been measured recently. We applied our GW-ITEP FSI corrections, covering a broad energy range up to  $E = 2.7$  GeV [6], to the CLAS Collaboration ( $E = 1050 - 2700$  MeV and  $\theta = 32^\circ - 157^\circ$ ) [11] and A2 Collaboration at MAMI ( $E = 301 - 455$  MeV and  $\theta = 45^\circ - 125^\circ$ ) [12]  $\gamma d \rightarrow \pi^- pp$  measurements to get elementary cross sections for  $\gamma n \rightarrow \pi^- p$ . In particular, the new CLAS cross sections have quadrupled the world database for  $\gamma n \rightarrow \pi^- p$  above  $E = 1$  GeV. The FSI correction factor for the CLAS and A2 kinematics was found to be small,  $\Delta\sigma/\sigma < 10\%$ .

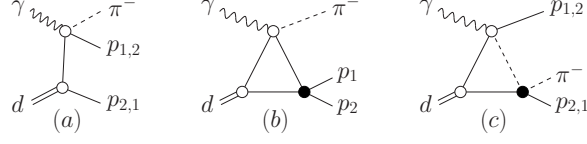


**FIGURE 3.** Feynman diagrams for the leading components of the  $\gamma d \rightarrow \pi^- pp$  amplitude. (a) Impulse approximation (IA), (b) pp-FSI, and (c)  $\pi N$ -FSI. Filled black circles show FSI vertices. Wavy, dashed, solid, and double lines correspond to the photons, pions, nucleons, and deuterons, respectively.

Obviously, CLAS and A2 measurements are not enough to have compatible proton and neutron databases, specifically the energy binning of the CLAS measurements is 50 MeV or, in the worst case, 100 MeV while A2 Collaboration at MAMI measurements are able to have 2 to 4 MeV binning.

### Neutron Data from Measurements with Deuteron Target

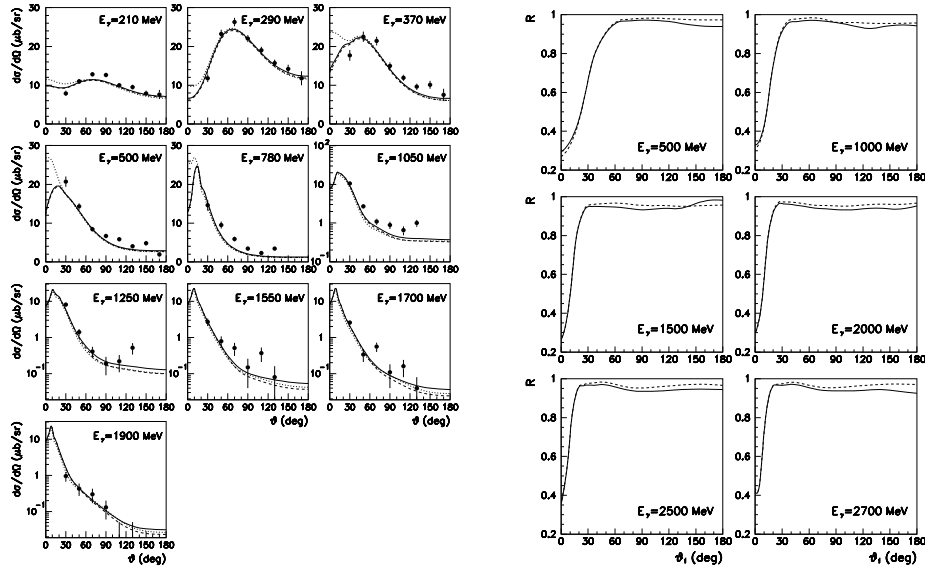


**FIGURE 4.** **Left panel:** The differential cross section,  $d\sigma_{\gamma d}/d\Omega$ , of the reaction  $\gamma d \rightarrow \pi^- pp$  in the laboratory frame at different values of the photon laboratory energy  $E < 1900$  MeV;  $\theta$  is the polar angle of the outgoing  $\pi^-$ . Dotted curves show the contributions from the IA amplitude [Fig. 3(a)]. Successive addition of the NN-FSI [Fig. 3(b)] and  $\pi N$ -FSI [Fig. 3(c)] amplitudes leads to dashed and solid curves, respectively. The filled circles are the data from DESY bubble chamber [16]. **Right panel:** The correction factor  $R(E, \theta)$ , where  $\theta$  is the polar angle of the outgoing  $\pi^-$  in the rest frame of the pair  $\pi^- +$  fast proton. The kinematic cut,  $P_p > 200$  MeV/c, is applied. The solid (dashed) curves are obtained with both  $\pi N$ - and NN-FSI (only NN-FSI) taken into account.

The determination of the  $\gamma d \rightarrow \pi^- pp$  differential cross sections with the FSI, taken into account (including all leading diagrams given in Fig. 3), were done recently [6, 11, 12], for the CLAS [11] and MAMI [12] data. The SAID of GW Data Analysis Center (DAC) phenomenological amplitudes for  $\gamma N \rightarrow \pi N$  [13],  $NN \rightarrow NN$  [14], and  $\pi N \rightarrow \pi N$  [3] were used as inputs to calculate the diagrams in Fig. 3. The Bonn potential (full model) [15] was used for the deuteron description. In Refs. [11, 12], we calculated the FSI correction factor  $R(E, \theta)$  dependent on photon energy,  $E$ , and pion production angle in CM frame  $\theta$  and fitted recent CLAS and MAMI  $d\sigma/d\Omega$  versus the world  $\gamma N \rightarrow \pi N$  database [9] to get new neutron multipoles and determine neutron resonance EM couplings [11].

Results of calculations and comparison with the experimental data on the differential cross sections,  $d\sigma_{\gamma d}/d\Omega$ , where  $\Omega$  and  $\theta$  are solid and polar angles of outgoing  $\pi^-$  in the laboratory frame, respectively, with z-axis along the photon beam for the reaction  $\gamma d \rightarrow \pi^- pp$  are given in Fig. 4 (left panels) for a number of the photon energies,  $E$ .

The FSI corrections for the CLAS and MAMI quasi-free kinematics were found to be small, as mentioned above. As an illustration, Fig. 4 (right panels) shows the FSI correction factor  $R(E, \theta) = (d\sigma/d\Omega_{\pi p})/(d\sigma^{IA}/d\Omega_{\pi p})$  for the  $\gamma n \rightarrow \pi^- p$  differential cross sections as a function of the pion production angle in the CM ( $\pi - p$ ) frame,  $\theta$ , for different energies over the range of the CLAS experiment. Overall, the FSI correction factor  $R(E, \theta) < 1$ , while the effect, i.e., the  $(1 - R)$  value, vary from 10% to 30%, depending on the kinematics, and the behavior is very smooth versus pion production angle. We found a sizeable FSI-effect from S-wave part of pp-FSI at small angles. A small but systematic effect  $|R - 1| \ll 1$  is found in the large angular region, where it can be estimated in the Glauber approach, except for narrow regions close to  $\theta \sim 0^\circ$  or  $\theta \sim 180^\circ$ . The  $\gamma n \rightarrow \pi^0 n$  case is much more complicated vs.  $\gamma n \rightarrow \pi^- p$  because in IA  $\pi^0 n$  final state can come from both  $\gamma n$  and  $\gamma p$  initial interactions [17]. The leading diagrams for  $\gamma d \rightarrow \pi^0 pn$  are similar as given on Fig. 3.

## New Neutron Amplitudes and Neutron EM Couplings

The solution, SAID GB12 [11], uses the same fitting form as SAID recent SN11 solution [18], which incorporated the neutron-target CLAS  $d\sigma/d\Omega$  for  $\gamma n \rightarrow \pi^- p$  [11] and GRAAL  $\Sigma$ s for both  $\gamma n \rightarrow \pi^- p$  [19] and  $\gamma n \rightarrow \pi^0 n$  [20]. This fit form was motivated by a multichannel K-matrix approach, with an added phenomenological term proportional to the  $\pi N$  reaction cross section.

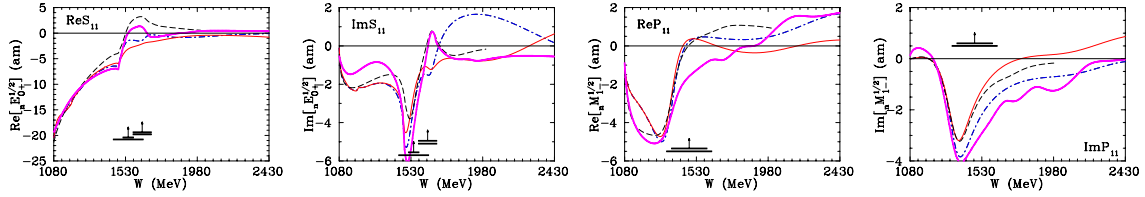


**FIGURE 5.** Samples of neutron multipoles for  $I = 1/2$ . Solid (dash-dotted) lines correspond to the SAID GB12 [11] (SN11 [18]) solution. Thick solid (dashed) lines give SAID GZ12 [11] solution (MAID07 [21]). Vertical arrows indicate mass (WR), and horizontal bars show full,  $\Gamma$ , and partial,  $\Gamma_{\pi N}$ , widths of resonances extracted by the Breit-Wigner fit of the  $\pi N$  data associated with the SAID solution WI08 [3].

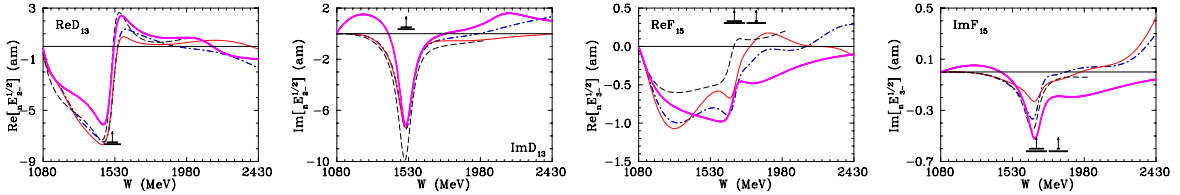


**FIGURE 6.** Samples of neutron multipoles for  $I = 3/2$ . Notation as in Fig. 5

However, these new CLAS cross sections departed significantly from our predictions at the higher energies, and greatly modified PWA result [11] (Figs. 5 and 6). Following that, the BnGa group reported a neutron EM coupling determination [22] using the CLAS Collaboration  $d\sigma/d\Omega$  with our FSI [11] (Table 1). BnGa13 [22] and SAID GB12 [11] used the same (almost) data [11] to fit them while BnGa13 has several new Ad-hoc resonances [1].

Overall: the difference between MAID07 [21] with BnGa13 and SAID GB12 is rather small but resonances may be essentially different (Table 1). The new BnGa13 has some difference vs. SAID GB12, PDG14 [1], for instance, for  $N(1535)1/2^-$ ,  $N(1650)1/2^-$ , and  $N(1680)5/2^+$ .

## Work in Progress

At MAMI in March of 2013, we collected deuteron data below  $E = 800$  MeV with 4 MeV energy binning [25] and will have a new experiment below  $E = 1600$  MeV [26] in the fall of 2016.

**TABLE 1.** Neutron helicity amplitudes  $A_{1/2}$  and  $A_{3/2}$  (in  $[(\text{GeV})^{-1/2} \times 10^{-3}]$  units) from the SAID GB12 [11] (first row), previous SAID SN11 [18] (second row), recent BnGa13 by the Bonn-Gatchina group [22] (third row), recent Kent12 by the Kent State Univ. group [23] (forth row), and average values from the PDG14 [1] (fifth row). The relativized quark model predictions came from Ref. [24] (sixth row).

Resonance	$nA_{1/2}$	Resonance	$nA_{1/2}$	$nA_{3/2}$	Ref.
N(1535)1/2 <sup>-</sup>	$-58 \pm 6$	N(1520)3/2 <sup>-</sup>	$-46 \pm 6$	$-115 \pm 5$	SAID GB12
	$-60 \pm 3$		$-47 \pm 2$	$-125 \pm 2$	SAID SN11
	$-93 \pm 11$		$-49 \pm 8$	$-113 \pm 12$	BnGa13
	$-49 \pm 3$		$-38 \pm 3$	$-101 \pm 4$	Kent12
	$-46 \pm 27$		$-59 \pm 9$	$-139 \pm 11$	PDG14
	-63		-38	-114	Cap92
N(1650)1/2 <sup>-</sup>	$-40 \pm 10$	N(1675)5/2 <sup>-</sup>	$-58 \pm 2$	$-80 \pm 5$	SAID GB12
	$-26 \pm 8$		$-42 \pm 2$	$-60 \pm 2$	SAID SN11
	$+25 \pm 20$		$-60 \pm 7$	$-88 \pm 10$	BnGa13
	$+11 \pm 2$		$-40 \pm 4$	$-68 \pm 4$	Kent12
	$-15 \pm 21$		$-43 \pm 12$	$-58 \pm 13$	PDG14
	-35		-35	-51	Cap92
N(1440)1/2 <sup>+</sup>	$+48 \pm 4$	N(1680)5/2 <sup>+</sup>	$+26 \pm 4$	$-29 \pm 2$	SAID GB12
	$+45 \pm 15$		$+50 \pm 4$	$-47 \pm 2$	SAID SN11
	$+43 \pm 12$		$+34 \pm 6$	$-44 \pm 9$	BnGa13
	$+40 \pm 5$		$+29 \pm 2$	$-59 \pm 2$	Kent12
	$+40 \pm 10$		$+29 \pm 10$	$-33 \pm 9$	PDG14
	-6		+19	-23	Cap92

New 589  $d\sigma/d\Omega$ s by the A2 Collaboration at MAMI contribution is about 160% to the previous world  $\pi^0 n$  database. Experiment is to have 19 angular  $d\sigma/d\Omega$  for  $-0.9 < \cos\theta < +1$  and 31 energy bins for  $E = 180 - 800$  MeV,  $\Delta E = 20$  MeV ( $W = 1105 - 1545$  MeV,  $\Delta W = 10$  MeV). Relative error of our measurement has a level of 1.5 – 3%. Preliminary data for total cross section of the reaction  $\gamma n \rightarrow \pi^0 n$  shown on Fig. 7. This measurement is compared

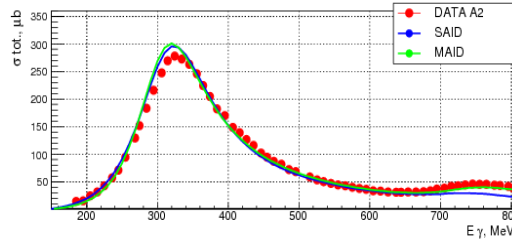


**FIGURE 7.** Preliminary total cross sections for  $\gamma n \rightarrow \pi^0 n$ . See text for details.

with a phenomenological result came from SAID [11] and MAID [21] PWAs. Comparison of our A2 Collaboration at MAMI experimental data with a MAID prediction gives more reasonable agreement, especially at higher energies.

Let us stress that the FSI corrections for the  $\pi^0$  photoproduction cross sections off the protons and neutrons are not equal in a general case. However, in a special case of the  $\Delta(1232)3/2^+$  energy region, the FSI corrections for  $\gamma p \rightarrow \pi^0 p$  and  $\gamma n \rightarrow \pi^0 n$  cross sections are equal due to the isospin structure of the  $\gamma N \rightarrow \pi N$  amplitude [17].

We are going to use our FSI technology to apply for the upcoming JLab CLAS (g13 run period)  $d\sigma/d\Omega$  for  $\gamma n \rightarrow \pi^- p$  covering  $E = 400 - 2500$  MeV and  $\theta = 18^\circ - 152^\circ$  [27]. This data set will bring about 11k new measurements which quadruple the world  $\gamma n \rightarrow \pi^- p$  database. The ELPH facility at Tohoku Univ. will bring new  $d\sigma/d\Omega$  for  $\gamma n \rightarrow \pi^0 n$  below  $E = 1200$  MeV [28].

## Conclusion

- The differential cross section for the processes  $\gamma n \rightarrow \pi^- p$  was extracted from new CLAS and MAMI-B measurements accounting for Fermi motion effects in the IA as well as NN- and  $\pi$ N-FSI effects beyond the IA.
- Consequential calculations of the FSI corrections, as developed by the GW-ITEP Collaboration, was applied.
- New cross sections departed significantly from our predictions, at the higher energies, and greatly modified the fit result.
- New  $\gamma n \rightarrow \pi^- p$  and  $\gamma n \rightarrow \pi^0 n$  data will provide a critical constraint on the determination of the multipoles and EM couplings of low-lying baryon resonances using the PWA and coupled channel techniques.
- Polarized measurements at JLab/JLab12, MAMI, SPring-8, CBELSA, and ELPH will help to bring more physics in.
- FSI corrections need to evaluate.

## Acknowledgments

This material is based upon work supported by the U.S. Department of Energy, Office of Science, Office of Nuclear Physics, under Award Number DE-FG02-99-ER41110.

## REFERENCES

- [1] K.A. Olive *et al.* (Particle Data Group Collaboration), *Chin. Phys. C* **38**, 090001 (2014).
- [2] K.M. Watson, *Phys. Rev.* **95**, 228 (1954); R.L. Walker, *Phys. Rev.* **182**, 1729 (1969).
- [3] R.A. Arndt, W.J. Briscoe, I.I. Strakovsky, and R.L. Workman, *Phys. Rev. C* **74**, 045205 (2006).
- [4] Ya.I. Azimov and I.I. Strakovsky, *Proceedings of the XVth International Conference on Hadron Spectroscopy* (Hadron 2013), Nara, Japan, Nov. 2013, PoS (Hadron 2014) 034.
- [5] A.B. Migdal, *JETP* **1**, 2 (1955); K.M. Watson, *Phys. Rev.* **88**, 1163 (1952).
- [6] V.E. Tarasov, W.J. Briscoe, H. Gao, A.E. Kudryavtsev, and I.I. Strakovsky, *Phys. Rev. C* **84**, 035203 (2011).
- [7] J. Hadamard, *Sur les problemes aux derivees partielles et leur signification physique*, (Princeton Univ. Bulletin. p. 49, 1902); A.N. Tikhonov and V.Y. Arsenin, *Solutions of Ill-Posed Problems*, (New York: Winston, 1977).
- [8] A.M. Sendorfi *et al.*, *AIP Conf. Proc.* **1432**, 219 (2012); K. Nakayama, private communication, 2014.
- [9] W.J. Briscoe, I.I. Strakovsky, and R.L. Workman, Institute of Nuclear Studies of The George Washington University Database; [http://gwdac.phys.gwu.edu/analysis/pr\\_analysis.html](http://gwdac.phys.gwu.edu/analysis/pr_analysis.html).
- [10] A. Shafi *et al.*, *Phys. Rev. C* **70**, 035204 (2004).
- [11] W. Chen *et al.*, *Phys. Rev. C* **86**, 015206 (2012).
- [12] W.J. Briscoe *et al.*, *Rev. C* **86**, 065207 (2012).
- [13] M. Dugger *et al.* (CLAS Collaboration), *Phys. Rev. C* **76**, 025211 (2007).
- [14] R.A. Arndt, W.J. Briscoe, I.I. Strakovsky, and R.L. Workman, *Phys. Rev. C* **76**, 025209 (2007).
- [15] R. Machleidt, K. Holinde, and C. Elster, *Phys. Rep.* **149**, 1 (1987).
- [16] P. Benz *et al.* (Aachen-Bonn-Hamburg-Heidelberg-Muenchen Collaboration), *Nucl. Phys. B* **65**, 158 (1973).
- [17] V. Tarasov *et al.*, to be published in *Phys. At. Nucl.* **79** (2016) ; arXiv:1503.06671 [hep-ph].
- [18] R.L. Workman *et al.*, *Phys. Rev. C* **85**, 025201 (2012).
- [19] G. Mandaglio *et al.* (GRAAL Collaboration), *Phys. Rev. C* **82**, 045209 (2010).
- [20] R. Di Salvo *et al.* (GRAAL Collaboration), *Eur. Phys. J. A* **42**, 151 (2009).
- [21] D. Drechsel, S.S. Kamalov, and L. Tiator, *Eur. Phys. J. A* **34**, 69 (2007).
- [22] A. Anisovich *et al.*, *Eur. Phys. J. A* **49**, 67 (2013).
- [23] M. Shrestha and D.M. Manley, *Phys. Rev. C* **86**, 055203 (2012).
- [24] S. Capstick, *Phys. Rev. D* **46**, 2864 (1992).
- [25] *Meson production off the deuteron. I*, Spokespersons: W.J. Briscoe and I.I. Strakovsky (A2 Collaboration at MAMI), MAMI Proposal MAMI-A2-02/12, Mainz, Germany, 2012.
- [26] *Meson production off the deuteron. II*, Spokespersons: W.J. Briscoe, V.V. Kulikov, K. Livingston, and I.I. Strakovsky (A2 Collaboration at MAMI), MAMI Proposal MAMI-A2-02/13, Mainz, Germany, 2013.
- [27] P. Mattione, *Proceedings of the XVth International Conference on Hadron Spectroscopy* (Hadron 2013), Nara, Japan, Nov. 2013, PoS (Hadron 2014) 096.
- [28] T. Ishikawa *et al.*, *Proceedings of the XVth International Conference on Hadron Spectroscopy* (Hadron 2013), Nara, Japan, Nov. 2013, PoS (Hadron 2014) 095.